International Journal of Engineering Trends and Technology
ISSN: 2231 – 5381 /doi:10.14445/22315381/IJETT-V70I2P226

Volume 70 Issue 2, 221-228, February, 2022

Original Article

Classification of Benign and Malignant MRIs using SVM Classifier for Brain Tumor Detection

Ibrahima Sory keita[1], Ir.Pratap Nair[2], Haarindra Prasad[3], Sudhakara pandian[4], S.Deivasigamani[5]

[1,2,3,5]*Faculty of Engineering& Computer Technology, AIMST University, Malaysia*
[4]*Department of Manufacturing Engineering, VIT University, Vellore Campus, India.*

[1]ibrahimasorykeita47@yahoo.fr, [2]pratap_n@aimst.edu.my, [3]haarindra@aimst.edu.my, [4]sudhakarapandian.r@vit.ac.in, [#5]deivasigamani@aimst.edu.my

Abstract *— A brain tumor is a clump of malformed tissue in which the cells proliferate rapidly and uncontrollably. Differentiating brain tumors from other brain tissue is critical for clinical diagnosis and therapy methods. This article presented a method for detecting and classifying brain tumor cells using a machine learning algorithm based on the Discrete Wavelet Transform (DWT). Additionally, characteristics from 2D DWT components are retrieved for the categorization of Benign (Be) and Malignant (Ma) Magnetic resonance imaging (MRI). After that, the features are trained and classified using the kernel Support Vector Machine (SVM) classification method. The proposed method stated in this work obtains 99% of accuracy (ACC), 99.14% of sensitivity (Se), and 98.79 % of specificity (Sp) concerning the MRI ground truth images.*

Keywords — *Benign and malignant, Brain tumor, DWT, MR images, Neural networks, SVM.*

I. INTRODUCTION

The brain is the central nervous system's control centre. The brain is a complicated organ because it includes between 50 and 100 billion neurons that create a massive network. A brain tumor is a collection of abnormal cells that develop either inside or outside the brain, which are classified as benign or malignant, with benign tumors being noncancerous and malignant tumors being cancerous [1]. Benign tumors are less damaging than malignant tumors because malignant tumors spread fast, infecting other brain regions and gradually deteriorating the condition until death occurs. Brain tumor identification is a difficult challenge for physicians to solve owing to the brain's complicated anatomy. By segmenting necrotic and augmented cells, the precise border should be determined for optimal therapy. Regardless of the type of treatment used, such as chemotherapy, radiation, or brain surgery, it is necessary to establish the exact location and extent of the brain tumor and any other afflicted areas. To do this, medical practitioners can utilize automated or semi-automatic equipment for brain tumor segmentation to assist them in adequately identifying the brain tumor before executing the operations. Medical imaging is a critical component of scientific study nowadays. Numerous medical instruments have been created in recent years to offer specific sectoral views of the human body. "Computed Tomography (CT) and Magnetic Resonance Imaging (MRI)" are the two most frequently utilized methods for visualizing human anatomy [2]. The MRI is one of the most often used imaging diagnostic tools for the human brain, as various tumors vary in shape and size [3]. With computer-aided system design, medical imaging techniques give automated ways for conducting segmentation algorithms. This technology produces treatment programs and imaging devices that physicians may use as more effective diagnostic tools. The primary goal of this study is to increase global awareness of brain tumors and simplify the screening procedure for brain tumor detection methods. At the moment, the expense of screening for brain tumors and a shortage of ineffective doctors in underdeveloped nations will erode the approach for detecting brain tumors. This article discusses the most cost-effective method for screening the brain tumor area for cancer illness. The primary contribution is the development of "an automated method for classifying brain tumor images as benign or malignant for future treatment" [4]. The approach presented in this article will assist clinicians in detecting and diagnosing brain disorders in significant populations. Recent years have seen a surge in interest in the subject of image analysis, which is becoming increasingly necessary. Numerous classification techniques have been investigated in this context, including Fuzzy C-means clustering [5], SVM with radial basis function [6], Convolutional Neural Network (CNN) [7], Deep CNN [8], SVM [9–11], Local Independent Projection-based classification [12], and Artificial Neural Network (ANN) [13].

The literature mentioned above indicated that specific approaches were created only for segmentation; others were invented solely for feature extraction, yet others were invented solely for classification. Additionally, because just a few characteristics are retrieved, the accuracy, sensitivity, and specificity for tumor identification are poor. We employed ten different characteristics in this investigation to get a greater level of accuracy. To increase diagnostic accuracy, we use a mix of biologically inspired DWT and kernel SVM as a classifier tool in this work. This work aims to collect data from segmented tumor regions and identify healthy and infected tumor tissues

using an open data set. The primary goal of this study is to raise global awareness of tumor disease and simplify the screening procedure for brain detection methods. Currently, the cost of screening for brain tumor disease and a shortage of inefficient doctors in underdeveloped nations are eroding the approach for tumor identification. This article discusses the most cost-effective methods for screening the tumor area of the brain for brain illness. The primary contribution is developing an automated process for classifying MR images into benign or malignant for further processing. The approach described in this article will assist radiologists in detecting and diagnosing abnormalities in the brain during extensive population screening. This study is structured as follows: Section 2 discusses the material and recommended technique. Section 3 details the experimental conditions and findings. Part 4 discusses the concluding section.

II. MATERIALS AND METHODS

A. Materials

The MR images used to evaluate the classification performance of brain tumors are obtained from the "Kaggle and Multimodal Brain Tumor Image Segmentation (BRATS) datasets (Brain web Database, http://www.bic.mni.mcgill.ca/brainweb>)". The collection included MRI brain images with a resolution of 512x512 in the axial, coronal, and sagittal planes. The images from this open access dataset are divided into training and testing sets in this article. The collection contains aberrant MRI brain images associated with glioma and meningioma disorders. 100 MRIs were selected for training purposes, with 40 benign, 40 malignant, and 20 normal brains.

B. Methods

The training and testing modes of the proposed approach for identifying benign and malignant MR images are depicted in Figure 1. Training is conducted in an offline format, while testing is conducted in an online mode. This training system uses a kernel SVM classifier in learning mode to train benign and malignant MR images. The suggested method is divided into three stages: preprocessing (using high-pass and median filters), feature extraction (using DWT and K-means segmentation), and classification (Kernel-SVM). The Kernel SVM is used in training mode to generate a learned pattern from benign and malignant MRI data. This learned pattern is utilized in the kernel SVM classification model to categorize MRI scans as benign or malignant. Figure 1(B) depicts the proposed MRI image categorization system in testing mode. DWT is used to convert the collected images to the frequency domain. Additionally, the characteristics of this modified MRI image are retrieved, and these images are categorized using a kernel SVM classifier (Classification mode) using the learned patterns.

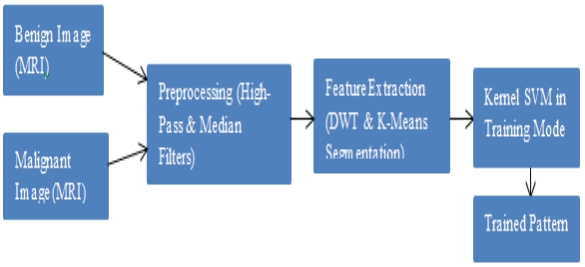

Fig. 1(a): Training mode-Proposed flow for image classification

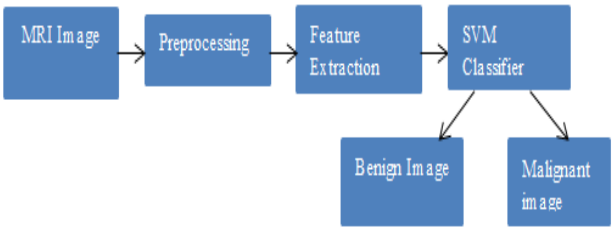

Fig. 2(b): Testing mode-Proposed flow for image classification

a) Preprocessing: Preprocessing is the initial stage of this research. MR images are smoothed and sharpened further using Gaussian high pass filter as shown in Equation (1) method to make them visible to the naked human eye to detect and identify tumors in the image and it [14].

$$H(u,v) = 1 - e^{-D^2(u,v)/2D_0^2} \quad (1)$$

Where $\begin{cases} u \text{ is matrices consisting of rows} \\ v \text{ is matrices consisting of columns} \\ D_0 \text{ is the cut} - \text{off distance} \end{cases}$

b) Feature Extraction: When it comes to decision-making, feature extraction plays a major part. Table 1 illustrates some of the most salient first- and second-order statistical analysis characteristics for normal and up to normal brain images, respectively. The proposed system was implemented by the DWT feature extraction method that consists of extracting statistical features from MR images. DWT tool is used for signal analysis which decomposes the image into different frequency (time to frequency) domains. The extracted features are then submitted to a classifier, which classifies based on these features. In this paper, the MR images are subjected to the 2D-DWT components for up to two levels of decomposition and as shown in Figure 2. f(a,b) indicates the picture's 2D function, h(i) denotes the intensity level, 'N' is the total number of grey levels in the image, and p(i) defines the probability density. The following equations [15] represent "p(i), h(i), f(a,b), and (i,j)" as shown in Equation (2-5).

$$p(i) = \frac{h(i)}{N_a N_b}, i = 0,1,2 \ldots N-1 \quad (2)$$

Where $\begin{cases} N \text{ is the total number of grey level} \\ h(i) \text{ is the intensity level} \\ P(i) \text{ is the probability density} \end{cases}$

$$h(i) = \sum_{x=0}^{N}\sum_{y=0}^{N-1} x(f(a,b),i) \qquad i = 0,1,2....N-1$$

(3) Where $\begin{cases} N \text{ is the total number of grey level} \\ h(i) \text{ is the intensity level} \\ f(a,b) \text{indicates image 2D function} \end{cases}$

$$x(i,j) = \begin{cases} 1; i = j \\ 0; i = j \end{cases} \quad (4)$$

$$f(a,b) = \text{median}\{g(i,j)\} \quad (5)$$

Where $\begin{cases} i \text{ is the scale matrix parameter} \\ j \text{ is the translate parameter} \\ f(a,b) \text{indicates image 2D function} \end{cases}$

1) Mean: Equation (6) indicates that the mean is defined as the image's average intensity level. It unambiguously establishes that the mean is a function of probability density [16].

$$\mu = \sum_{i=0}^{N-1} i.p(i) \quad (6)$$

Where $\begin{cases} N \text{ is the total number of grey level} \\ P(i) \text{is the probability density} \\ (i) \text{ is the scale matrix parameter} \end{cases}$

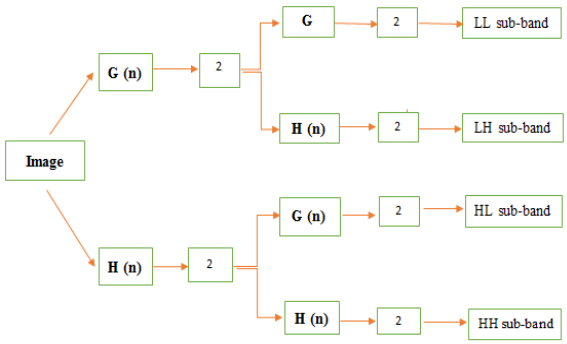

Fig. 2: Decomposition of an image using 2D DWT components

2) Standard Deviation (SD)*:* As demonstrated in Equation (16), the standard deviation is computed using the mean value of the pixels and their probability densities.

$$SD \text{ or } \sigma = \sqrt{\sum_{i=0}^{N-1}(i-\mu)^2.p(i)} \quad (7)$$

Where $\begin{cases} N \text{ is the total number of grey level} \\ P(i) \text{is the probability density} \\ (i) \text{is the scale matrix parameter} \\ \mu \text{ is the mean coefficient} \end{cases}$

3) Entropy: A random variable's entropy [16] value indicates its degree of uncertainty. It is proportional to the probability density p(i), as shown in Equation (8).

$$Entropy = -\sum_{i=0}^{N-1} p(i)\log_2[p(i)] \quad (8)$$

Where $\begin{cases} N \text{ is the total number of grey level} \\ P(i) \text{is the probability density} \\ (i) \text{ is the scale matrix parameter} \end{cases}$

4) Variance*:* The variance [16] is used to quantify intensity fluctuation. Additionally, as seen in Equation (9), it is calculated by squaring the standard deviation.

$$\sigma^2 = \sum_{i=0}^{N-1}(i-\mu)^2.p(i) \quad (9)$$

Where $\begin{cases} N \text{ is the total number of grey level} \\ P(i) \text{is the probability density} \\ (i) \text{is the scale matrix parameter} \\ \mu \text{ is the mean coefficient} \end{cases}$

5) Kurtosis*:* Kurtosis [16] is used to determine the flatness of the histogram. The mathematical representation of kurtosis as a function of standard deviation, mean, and probability density is shown in Equation (10).

$$\mu^4 = \sigma^4 \sum_{i=0}^{N-1}((i-\mu)^4.p(i)) - 3 \quad (10)$$

Where $\begin{cases} N \text{ is the total number of grey level} \\ P(i) \text{is the probability density} \\ (i) \text{is the scale matrix parameter} \\ \mu \text{ is the mean coefficient} \\ \sigma \text{ is the standard deviation coefficient} \end{cases}$

6) Skewness*:* The skewness of a picture defines its symmetry [9]. It is indicated by the μ3 and is illustrated in Equation (11).

$$\mu^3 = \sigma^{-3}\sum_{i=0}^{N-1}((i-\mu)^3.p(i)) \quad (11)$$

Where $\mu^3 < 0$; *Histogram below mean*
$\mu^3 = 0$; *Histogram is equal to mean*
$\mu^3 > 0$; *Histogram above mean*

Where $\begin{cases} N \text{ is the total number of grey level} \\ P(i) \text{is the probability density} \\ (i) \text{is the scale matrix parameter} \\ \mu \text{ is the mean coefficient} \\ \sigma \text{ is the standard deviation coefficient} \end{cases}$

7) Inverse Difference Moment (IDM): IDM [9] calculates an image's local homogeneity as stated in Equation (12).

$$IDM = \sum_{i=0}^{N-1}\sum_{i=0}^{N-1} \frac{1}{1+(i-j)^2} p(i,j) \quad (12)$$

Where $\begin{cases} i \text{ is the scale matrix parameter} \\ j \text{ is the translate parameter} \\ p(j,j) \text{ is the probability density} \\ N \text{ is the total number of grey level} \end{cases}$

8) Contrast: Contrast [9] determines the intensity fluctuation between the threshold and its closest pixel, as indicated in Equation (13).

$$Contrast = \sum_{n=0}^{N-1}\sum_{i=0}^{N-1}\sum_{j=0}^{N-1} p(i,j)^2 \quad (13)$$

Where $\begin{cases} i \text{ is the scale matrix parameter} \\ j \text{ is the translate parameter} \\ p(j,j) \text{ is the probability density} \\ N \text{ is the total number of grey level} \end{cases}$

9) Correlation: Correlation [9] is expressed analytically in Equation (14). It is used to determine the relationship between the threshold and the nearest pixel.

$$Correlation = \frac{1}{\sigma_a \sigma_b} \sum_{i=0}^{N-1} \sum_{j=0}^{N-1} (i,j).p(i,j)^2 - \mu_a \mu_b \quad (14)$$

Where $\begin{cases} i \text{ is the scale matrix parameter} \\ j \text{ is the translate parameter} \\ p(j,j) \text{ is the probability density} \\ N \text{ is the total number of grey level} \\ \sigma \text{ is the standard deviation coefficient} \\ \mu \text{ is the mean coefficient} \end{cases}$

10) Energy: Equation (15) denotes the mathematical representation of energy [9]. The energy is used to determine homogeneity. Additionally, it is referred to as the angular second moment or homogeneity.

$$Energy = \sum_{i=0}^{N-1} \sum_{j=0}^{N-1} p(i,j)^2 \quad (15)$$

Where $\begin{cases} i \text{ is the scale matrix parameter} \\ j \text{ is the translate parameter} \\ p(j,j) \text{ is the probability density} \\ N \text{ is the total number of grey level} \end{cases}$

11) Segmentation: The following algorithm describes how the K-means clustering method works:

- Indicate the number of clusters K. Initialize centroids by shuffling the dataset first and then randomly picking K data points without replacement for the centroids.
- Continue iterating until the centroids remain unchanged. i.e., the clustering of data points remains constant. Assume that X = x1, x2,..., xn is the set of data points and V = v1, v2,..., vc is the set of centers.
- At random, choose 'c' cluster centers. Determine the distance between each data point and the cluster nodes.
- Assign the data point to the cluster center with the shortest distance between it and other cluster centers. Utilize Equation (16) to recalculate the new cluster center:

$$v_i = \left(\frac{1}{C_i}\right) \sum_{j=1}^{ci} x_i \quad (16)$$

(Where 'c_i' represents the number of data points in the ith cluster)

1) Classification: Classification is critical in identifying benign and malignant MR images. The classifier divides the test MR images into benign and malignant images representing regular brain activity and aberrant brain activity. The recovered features from the converted coefficients at the 2D DWT components sub-bands are taught in the classifier's training mode, and the same method is repeated for the test MRI pictures. Kernel SVM classifier is used in this study to classify brain MR images. SVM is predicated on the fundamental hazard minimization criterion associated with the measurable learning hypothesis. The section regulates the observational hazard and arrangement limit to maximize the margin between classes and minimize expenditures, as Anuja et al. indicate [17]. An SVM constructs an optimal hyperplane representation of the decision surface that optimizes the separation of two classes in the data. Support vectors are small subsets of training data that provide evidence for the decision surface's optimal position. Thus, kernel machines are a subclass of support vector machine learning methods that include transforming predictors (input data) into a high-dimensional feature space. The SVM is used to create an indication from a large amount of preparation data, where the capacity can be bidirectional, multi-classification, or even a general relapse indicator. The SVM constructs a hypersurface that attempts to partition the positive and negative models by the most significant possible margin on all sides of the hyperplane. Due to the direct detachable nature of the data, the linear SVM seeks to identify, among all hyperplanes that limit the preparation error, the one that separates the preparation data from their nearest foci in the best possible way (maximal margin hyperplane).

It performs a quadratic optimization problem to determine the optimal hyperplane and classify the modified features into two groups. The number of modified features is proportional to the number of support vectors. Only the support vectors selected from the training data are required to build the decision surface. Once trained, the remainder of the training data is superfluous. Equation (17) illustrates the Radial basis method kernel utilized in conjunction with SVM in this work.

$$K(x_1, x_2) = \exp\left(-\frac{|x1-x2|^2}{2\sigma^2}\right) \quad (17)$$

Where x_1 & x_2 are vectors of feature space, and σ is the width of the kernel?

C. Results and Discussions

The performance assessment method for benign and malignant MRI image classifications is critical for assessing the performance of the tumor disease classification system. The 2D-DWT transform is used to brain MR images to produce the set of transformed coefficients. A confusion matrix is a table commonly used to determine the efficacy of proposed frameworks in terms of metrics. The confusion matrix in Table 1 specifies the categorization performance metrics True positive (TP), True negative (TN), False positive (FP), and False negative (FN). The extracted feature values are shown in Table 3.

Table 1. Confusion matrix for MR image classification

Expected outcome results	(Predicted) Benign	(Predicted) Malignant	Row Total
Positive metric	82	1	83
Negative metric	1	116	117
Column Total	83	117	200

The following parameters [18] from the confusion matrix are used in this research work for the brain tumor detection system

$$Se = \frac{TP}{(TP+FN)} \quad (18)$$

$$Sp = \frac{TN}{(TN+FP)} \quad (19)$$

$$Precision = \frac{TP}{(TP+FP)} \quad (20)$$

Where,

$$T_1 = \sqrt{(TP+FN)(TP+FP)} \quad (21)$$

$$T_2 = \sqrt{(TN+FN)(TN+FP)} \quad (22)$$

Se, Sp, Acc, and Precision are computed for the collection of MR images. The parameters Se and Sp describe the ratio of benign to malignant MR images that are well-detected. "Acc" is the ratio of all benign or malignant MR images identified and categorized correctly. TP denotes the number of adequately recognized malignant images. TN denotes the number of correctly identified benign images, the number of incorrectly identified benign images is denoted by FP, and FN denotes the number of incorrectly identified malignant images.

The training set randomly picked 50 benign and 50 malignant MR images from the dataset, whereas the testing set consisted of 200 unknown images. The 116 malignant MRI pictures (TP) are accurately classified as tumor images, whereas the 82 benign MR images (TN) are classified correctly as non-tumor images. One non-tumor image (FP) is incorrectly classified as malignant, while one tumor image (FN) is incorrectly classified as benign. This article utilized Equations (18-22) and achieved results as 99.14% of Se, 98.79% of Sp, 99% of Acc, and 99.14% of precision, shown in Table 2.

The performance of the system is compared to the state of the art in Table 4. All tests were conducted on a desktop PC equipped with MATLAB R2014 and a 64-bit Intel(R) Core(TM) i3-6100HQ CPU running at 3.70GHz x 4GB RAM. The challenge database comprises images that have been wholly anonymized from publically accessible images, and a collection of 200 MRI scans was also chosen to test the system. Additionally, this collection comprises ground truth pictures, which are collected from an experienced radiologist.

Table 2. Parameter for evaluating the suggested methodology's performance

Variable	Results in %
Accuracy	99
Misclassification Rate	1
Sensitivity	99.14
Specificity	98.79
Precision	99.14

Numerous simulations were run, and the following findings are presented. The original picture that served as the basis for our investigation is seen in Figure 3. (A). The ground truth brain pictures are shown in Figure 3 (B), the tumor alone is shown in Figure 3 (C), and the tumor borders, malignant and benign images are shown in Figure 3(D) and Figure 3(E).

(23)

Table 3. First And Second Order Statistical And Textural Features For Few Images

Features	Mean		SD		Entropy		Variance		Kurtosis		skewness		IDM		Contrast		Correlation		Energy	
Images	Be	Ma	Be	Ma	Be	Ma	Be	Ma	Be	Ma	Be	Ma	Be	Ma	Be	Ma	Be	Ma	Be	Ma
Image 1	0.0021	0.005	0.0898	0.0898	3.5182	3.438	0.008	0.008	6.7672	9.7677	0.4413	0.8647	0.5462	-0.299	0.225	0.2597	0.0991	0.1777	0.7691	0.7743
Image 2	6.87E-04	0.0035	0.0898	0.0897	2.7465	3.5239	0.0081	0.008	10.9703	6.522	0.7365	0.4979	0.119	1.6524	0.2689	0.2517	0.0977	0.0734	0.7861	0.7402
Image 3	0.0028	0.0052	0.0898	0.0897	2.761	3.666	0.0081	0.008	15.4102	6.3381	1.3077	0.3885	0.4422	0.3653	0.292	0.2283	0.1564	0.1375	0.8216	0.746
Image 4	0.0032	0.0032	0.0898	0.0898	3.0514	3.3888	0.008	0.008	7.5267	9.8067	0.6199	0.9578	0.3309	0.7148	0.2522	0.285	0.1013	0.0939	0.7651	0.7775
Image 5	0.0039	0.0051	0.0897	0.0897	3.1027	3.2353	0.008	0.008	7.6727	21.9671	0.5695	2.106	0.058	2.2563	0.2589	0.3379	0.0616	0.062	0.7464	0.7846
Image 6	0.0037	0.0039	0.0897	0.0897	2.768	3.1394	0.0081	0.008	19.2615	10.9158	1.6753	0.9919	-0.855	0.5923	0.302	0.3006	0.1209	0.0785	0.7886	0.7486
Image 7	0.002	0.0026	0.0898	0.0898	3.0685	3.4676	0.0081	0.0081	7.6454	7.0363	0.5282	0.6442	-0.630	-0.121	0.2567	0.2506	0.0726	0.0677	0.7534	0.7496
Image 8	0.0043	0.0047	0.0897	0.0897	3.0808	3.1074	0.008	0.0081	7.1283	15.2118	0.7145	1.5659	-0.274	1.9924	0.2528	0.3223	0.1	0.1049	0.7388	0.7937
Image 9	0.0037	0.0057	0.0897	0.0896	3.3052	3.6473	0.008	0.008	6.3672	5.6318	0.559	0.3859	-0.399	1.0705	0.2464	0.2375	0.0704	0.0879	0.7354	0.7235
Image10	0.0029	0.0058	0.0898	0.0896	2.9381	3.6494	0.0081	0.0081	7.999	5.9642	0.7375	0.5184	-0.494	0.094	0.2514	0.2405	0.0943	0.1015	0.7551	0.7411
Normal Image																				
Image 1	0.0044		0.0897		3.4587		0.008		8.285		0.6312		1.1692		0.2403		0.1318		0.7746	
Image 2	0.0013		0.0898		2.5998		0.0081		11.9538		0.8983		-0.0326		0.27		0.1122		0.7794	
Image 3	0.0054		0.0897		2.225		0.0081		27.9199		2.6057		1.7647		0.4074		0.1024		0.8407	
Image 4	0.0031		0.0898		2.6673		0.0081		9.4202		0.778		0.0863		0.2728		0.1412		0.7701	
Image 5	0.0034		0.0898		2.6846		0.0081		8.3566		0.6391		0.0324		0.2661		0.1025		0.7603	

Table 4. Similarities of Results to State-of-the-Art Methods

Authors	Classifier	Methodology (R2.3)	Year	Se (%)	Sp(%)	Acc(%)
Proposed work	Kernel-SVM	DWT	2021	99.14	98.79	99
Hemanth G et al. [7]	Convolution Neural Network	Pixel Based Segmentation	2019	---	---	91
Nooshin Nabizadeh et al.[19]	RBF-Kernel SVM	Gabor-Wavelet Transform	2015	96.2	95.7	96.7
Reema Mathew et al.[10]	Artificial neural network classifier	DWT	2018	97.62	99.98	99.40
Javeera A et al. [11]	SVM	SVM Transforms	2020	91.9	98	97.1
Banerjee S et al.[12]	Convolution Neural Network	Leave-one-patient-out Test	2019	--	---	97
Zhang Y et al.[20]	Kernel-SVM	Principle Component Analysis	2012	---	---	99.38
Agarap M [21]	Recurrent Neural Network	Gated Recurrent Unit	2018	---	---	84.15
Azar AT et al. [18]	SVM	Discrete methods	2012	97.08	98.90	97.71

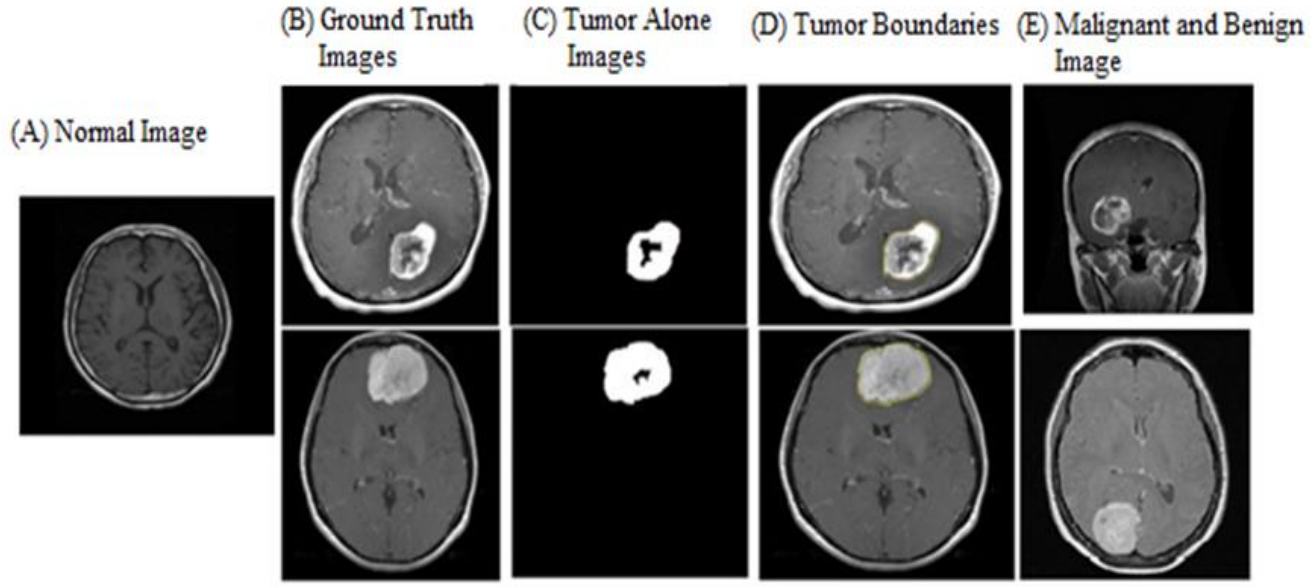

Fig. 3 Simulation Results

D. Results and Discussions

MR images are utilized to detect the tumor area in the brains of tumor patients. In this work, benign and malignant MR images are categorized automatically for tumor identification. DWT is used in this study to deconstruct MRI pictures into transformed coefficients. Additionally, the DWT coefficients are used to extract entropy, variance, mean, standard deviation, kurtosis, skewness, IDM, contrast, correlation, and energy characteristics. These characteristics are learned and categorized using a kernel-SVM classifier to identify the acquired MR images as benign or malignant. Automatic MRI image categorization achieves an average accuracy of around 99 percent. This study obtained a Se of 99.14, an Sp of 98.79, an accuracy of 99.14, and a precision of 99.14 percentages. Thus, the method described in this article may be utilized in brain tumor diagnostic centers to detect and diagnose tumor features in patients using a computer-assisted approach. Future work is focused on this area to predict the onset of seizure points in the EEG signals of epilepsy disorder patients.

REFERENCES

[1] Iqbal S, Khan MUG, Saba T, Rehman A. Computer-assisted brain tumor type discrimination using magnetic resonance imaging features. Biomed Eng Lett. 8(1) (2018) 5–28.

[2] Sahoo L, Sarangi L, Dash BR, Palo HK. Detection and Classification of Brain Tumor Using Magnetic Resonance Images. Lect Notes Electr Eng. 665(1) (2020)429–41.

[3] Song G, Huang Z, Zhao Y, Zhao X, Liu Y, Bao M, et al. A Noninvasive System for the Automatic Detection of Gliomas Based on Hybrid Features and PSO-KSVM. IEEE Access.7 (2019)13842–55.

[4] Abd-Ellah MK, Awad AI, Khalaf AAM, Hamed HFA. A review on brain tumor diagnosis from MRI images: Practical implications, key achievements, and lessons learned. Magn Reson Imaging [Internet].61 (2018) 300–18. Available from: https://doi.org/10.1016/j.mri.2019.05.028

[5] Naz S, Majeed H, Irshad H. Image segmentation using fuzzy clustering: A survey. Proc - 2010 6th Int Conf Emerg Technol ICET. (2010) 181–6.

[6] Kang J, Ullah Z, Gwak J. Mri-based brain tumor classification using ensemble of deep features and machine learning classifiers. Sensors. 21(6) (2021)1–21.

[7] Hemanth G, Janardhan M, Sujihelen L. Design and implementing brain tumor detection using machine learning approach. Proc Int Conf Trends Electron Informatics, ICOEI . (2019) 1289–94.

[8] Banerjee S, Mitra S, Masulli F, Rovetta S. Brain tumor detection and classification from multi-sequence MRI: study using convnets. Lect Notes Comput Sci (including Subser Lect Notes Artif Intell Lect Notes Bioinformatics). 11383 (2019)170–9.

[9] Bahadure NB, Ray AK, Thethi HP. Image Analysis for MRI Based Brain Tumor Detection and Feature Extraction Using Biologically Inspired BWT and SVM. Int J Biomed Imaging.(2017).

[10] Reema Mathew A, Babu Anto P, Thara NK. Brain tumor segmentation and classification using DWT, Gabour wavelet and GLCM. 2017 Int Conf Intell Comput Instrum Control Technol ICICICT .(2018) 1744–50.

[11] Amin J, Sharif M, Yasmin M, Fernandes SL. A distinctive approach in brain tumor detection and classification using MRI. Pattern Recognit Lett [Internet]. 139 (2020) 118–27. Available from: https://doi.org/10.1016/j.patrec.2017.10.036

[12] Huang M, Yang W, Wu Y, Jiang J, Chen W, Feng Q. Brain tumor segmentation based on local independent projection-based classification. IEEE Trans Biomed Eng.61(10) (2014) 2633–45.

[13] Faisal Z, El Abbadi NK. Detection and recognition of brain tumor based on DWT, PCA and ANN. Indones J Electr Eng Comput Sci.18(1) (2019) 56–63.

[14] Makandar A, Halalli B. Image Enhancement Techniques using Highpass and Lowpass Filters. Int J Comput Appl. 109(14) (2015) 21–7.

[15] Zulpe N, Pawar V. GLCM textural features for Brain Tumor Classification. Int J Comput Sci Issues. 9(3) (2012) 354–9.

[16] Shingare K V, N. D. P. An Efficient Brain Image Classification Using Probabilistic Neural Network and Tumor Detection Using Image Processing. IJARCCE. 4(5) (2014)631–8.

[17] Anuja SB, K UN, Sukanya ST. ECG Signals Classification using Statistical and Wavelet Features. Int J Recent Technol Eng. 8(5) (2020)1497–504.

[18] Azar AT, El-Said SA. Performance analysis of support vector machines classifiers in breast cancer mammography recognition. Neural Comput Appl.24(5) (2014) 1163–77.

[19] El Kader IA, Xu G, Shuai Z, Saminu S. Brain Tumor Detection and Classification by Hybrid CNN-DWA Model Using MR Images. Curr Med Imaging Former Curr Med Imaging Rev. (2021) 17.

[20] Nabizadeh N, Kubat M. Brain tumors detection and segmentation in MR images: Gabor wavelet vs statistical features. Comput Electr Eng [Internet]. 45 (2015) 286–301. Available from: http://dx.doi.org/10.1016/j.compeleceng.2015.02.007

[21] Zhang Y et al. Progress In Electromagnetics Research, 130 (2012) 369–388, 2012. Prog Electromagn.

[22] Agarap AFM. A neural network architecture combining gated recurrent unit (GRU) and support vector machine (SVM) for intrusion detection in network traffic data. ACM Int Conf Proceeding Ser. (2006) (2018) 26–30.